

Friction between a polyethylene pin and a microtextured CoCrMo disc, and its correlation to polyethylene wear, as a function of sliding velocity and contact pressure, in the context of metal-on-polyethylene prosthetic hip implants

A. Borjali, K. Monson, B. Raeymaekers*

Department of Mechanical Engineering, University of Utah, Salt Lake City, UT 84112, USA

ARTICLE INFO

Keywords:

Microtexture
Prosthetic hip implant
Patient-specific

ABSTRACT

The longevity of metal-on-polyethylene prosthetic hip implant bearings, in which a polished CoCrMo femoral head articulates with a polyethylene liner, is limited by mechanical instability or inflammation resulting from osteolysis caused by polyethylene wear debris. We use pin-on-disc experiments to measure friction and wear of a polyethylene pin that articulates with different microtextured CoCrMo surfaces, covering a wide range of operating conditions including sliding velocity and contact pressure. We determine how the lubrication regime changes as a function of operating conditions, and show that the microtexture accelerates the transition from boundary to elastohydrodynamic lubrication. Additionally, we illustrate that the microtexture could enable tailoring the hip implant to specific patient needs based on activity level, gender, and age.

1. Introduction

Total hip replacement (THR) surgery is used to treat degenerative joint diseases such as osteoarthritis, by replacing a patient's natural hip joint with a prosthetic implant. More than 300,000 THR surgeries are performed in the United States (US) each year (2015 data [1]). A prosthetic hip implant comprises a femoral head attached to a stem anchored in the femur bone, and articulates with an acetabular liner seated in an acetabular shell fixated in the pelvis [1]. The articulation between the femoral head and the acetabular liner restores the natural hip function of the patient.

Different types of prosthetic hip implant bearing material pairs exist, including metal-on-polyethylene (MOP), ceramic-on-polyethylene (COP), and ceramic-on-ceramic (COC). MOP prosthetic hip implants are the most common type used in the US, and consist of a cobalt chromium molybdenum (CoCrMo) alloy femoral head that articulates with a polyethylene acetabular liner, typically made of (Vitamin-E infused) highly cross-linked ultra-high molecular weight polyethylene (UHMWPE).

It is well-documented that the statistical survivorship of MOP prosthetic hip implants declines significantly after 15–25 years of use [2,3], primarily because of aseptic failure and instability (75%) [4], infection (7%) [5], and dislocation (6%) [6]. These failure mechanisms

are often driven by inflammatory response to microscopic, indigestible polyethylene wear debris, which may cause weakening of the bone (“osteolysis”) and, in turn, implant loosening and instability [5,7–9]. Approximately 10% of THR surgeries eventually result in a revision surgery [10], during which a failed prosthetic hip implant is replaced with a new one. A revision surgery is risky for the patient and costly for the healthcare system [11]. Thus, increasing longevity of MOP prosthetic hip implants, and particularly reducing polyethylene wear, is of critical importance.

Current approaches to increase longevity of prosthetic hip implants by reducing polyethylene wear involve improving the mechanical properties and wear resistance of the polyethylene acetabular liner, or changing the materials and design of the femoral head/acetabular liner pairs. For instance, the introduction of highly cross-linked polyethylene (HXPE), and subsequently vitamin-E infused HXPE, has resulted in a substantial reduction of polyethylene wear [12–16]. On the other hand, using new materials such as titanium [17], zirconia [18–20], silicon nitride [21], and tungsten [22], and manufacturing ultra-smooth ceramic bearing surfaces have also successfully reduced polyethylene wear [23].

A few researchers have pursued different approaches to reduce polyethylene wear, such as manufacturing a pattern of spherical microtexture features on the surface of commonly used femoral head materials, such as

* Corresponding author.

E-mail address: bart.raeymaekers@utah.edu (B. Raeymaekers).

<https://doi.org/10.1016/j.triboint.2018.07.005>

Received 27 March 2018; Received in revised form 15 June 2018; Accepted 3 July 2018

Available online 04 July 2018

0301-679X/ © 2018 Elsevier Ltd. All rights reserved.

CoCrMo and stainless steel [24–30]. Using traditional pin-on-disc (POD) and joint simulator experiments, these studies documented that friction and wear between a polyethylene pin and a CoCrMo surface with spherical microtexture features of diameter between 0.3 μm and 500 μm and depth between 0.25 μm and 100 μm , respectively, decreased on the order of 20–60%, compared to experiments with non-textured CoCrMo surfaces [24–26]. These studies concluded that the microtexture features served as lubricant reservoirs and accumulation areas for polyethylene wear debris. In contrast, other studies used shallow spherical microtexture features specifically designed to create microhydrodynamic bearings [28–30]. Chyr et al. [28] used a custom friction measurement apparatus with cylindrical CoCrMo microtextured and non-textured surrogate femoral head specimens articulating with conformal cylindrical UHMWPE specimens, mimicking the flexure/extension kinematics and axial loading of a hip joint. Borjali et al. [29], and Langhorn et al. [30] used POD wear experiments with different types of polyethylene pins articulating with microtextured and non-textured CoCrMo discs. In these studies, the patterned microtexture increased the lubricant film thickness that separates the bearing surfaces, thereby reducing contact, friction, and wear. No evidence was found that the microtexture features also accumulated polyethylene wear particles, likely because the microtexture features, when designed to create microhydrodynamic bearings, were too shallow. Langhorn et al. [30] also showed that the patterned microtexture does not negatively affect the corrosion potential of CoCrMo.

However, despite these efforts, no systematic study exists that quantifies the friction coefficient between polyethylene and microtextured CoCrMo specimens, and the corresponding polyethylene wear rate, as a function of operating conditions including contact pressure and sliding velocity. Since human hip kinematics and loading are functions of age, gender, body mass, and activity level [31–35], such results are crucial to understanding the effect of a patterned microtexture on polyethylene wear and, additionally, to using this information in the design of microtextured prosthetic hip implants. Ultimately, it could enable tailoring the patterned microtexture design to specific operating conditions, potentially finding application in patient-specific prosthetic hip implants accounting for age, gender, body mass, and activity level. Furthermore, no publications seem to exist that document the correlation between friction coefficient and polyethylene wear rate in POD experiments with a polyethylene pin and a microtextured CoCrMo disc, in the context of MOP prosthetic hip implants.

Hence, the objective of this paper is to experimentally measure the friction coefficient between a polyethylene pin and a CoCrMo disc with and without a patterned microtexture consisting of shallow concave texture features, as a function of operating conditions including contact pressure and sliding velocity. The patterned microtexture is specifically designed to create microhydrodynamic bearings, using theoretical models we have implemented and documented earlier [36]. We also correlate the friction coefficient measurements with the polyethylene wear rate, obtained in earlier experiments with identical operating conditions [29].

2. Materials and methods

2.1. Specimens

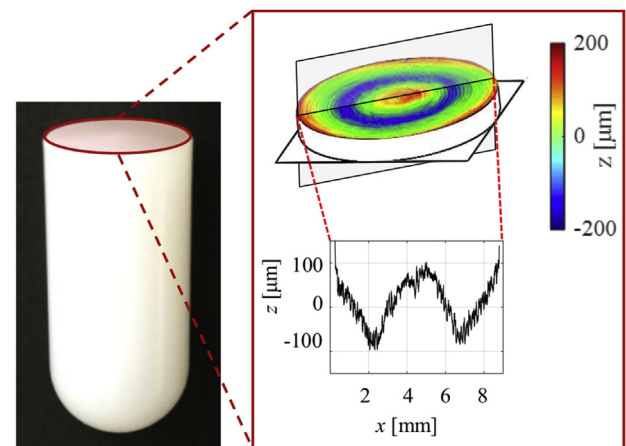
We evaluate two sets of polyethylene pins (diameter = 9 mm, length = 15 mm): (1) retrieved polyethylene pins from our previous wear study [29], and (2) virgin polyethylene pins. The retrieved polyethylene pins are machined from medical grade (1) UHMWPE GUR1050, (2) highly cross-linked polyethylene with 75 kGy gamma radiation (HXPE), and (3) vitamin-E infused highly cross-linked polyethylene with 75 kGy gamma radiation (VEXPE). These retrieved polyethylene pins have been subject to 2 million wear cycles with 2 MPa contact pressure and 1 Hz cycle frequency following a circular (diameter = 10 mm) wear path, using bovine calf serum with 20 mg/ml protein concentration as lubricant. The details of the wear experiments with these polyethylene pins are documented elsewhere [29]. The virgin polyethylene pins are machined from medical grade UHMWPE

GUR 1050 ram-extruded bar stock in accordance with the ASTM F648-14 standard [37]. Both retrieved and virgin polyethylene pins have identical geometry, with one flat end that articulates with the CoCrMo disc, and one hemispherical end that self-aligns the pin with the disc in a conical pin holder. The flat end of the pins is finished to average surface roughness $R_a < 5.5 \mu\text{m}$, which is similar to the surface finish of the polyethylene liner of commercial MOP prosthetic hip implants. Table 1 shows a virgin polyethylene pin and the surface topography of its flat articulating surface, measured using white light interferometry (Zygo NewView 5000). A trace along the diameter of the articulating surface illustrates the scale of the surface topography and reveals machining marks. Table 1 also shows R_a , R_q , and R_t values, and the asperity density n_s , mean radius of asperity summits R_s , and the standard deviation of asperity heights σ_s , determined from the white light interferometry data of the articulating surface, using a deterministic 8-nearest neighbor scheme [38]. This surface topography is typical for all virgin polyethylene pins, and for the retrieved pins prior to wear testing.

We evaluate five different patterned microtexture designs, selected based on our previous work [29], and specifically designed to create microhydrodynamic bearings. Table 2 lists the different spherical microtexture designs in terms of the texture density S_p , which represents the fraction of the bearing surface that is covered with microtexture features, and the texture aspect ratio ϵ , which is the ratio of the depth to the diameter of the spherical texture features. We use laser surface texturing (LST) with a femtosecond laser ablation process to manufacture the patterned microtexture designs on smooth CoCrMo discs (ASTM F1537-08 [39]). The CoCrMo discs are polished to $R_a < 50 \text{ nm}$, similar to the surface finish of femoral heads of commercial MOP prosthetic hip implants. A non-textured CoCrMo disc serves as a benchmark specimen. Table 2 shows an optical microscopy image, a 3D white light interferometry image of a single spherical texture feature, and a cross-sectional view along its centerline, for each CoCrMo disc,

Table 1

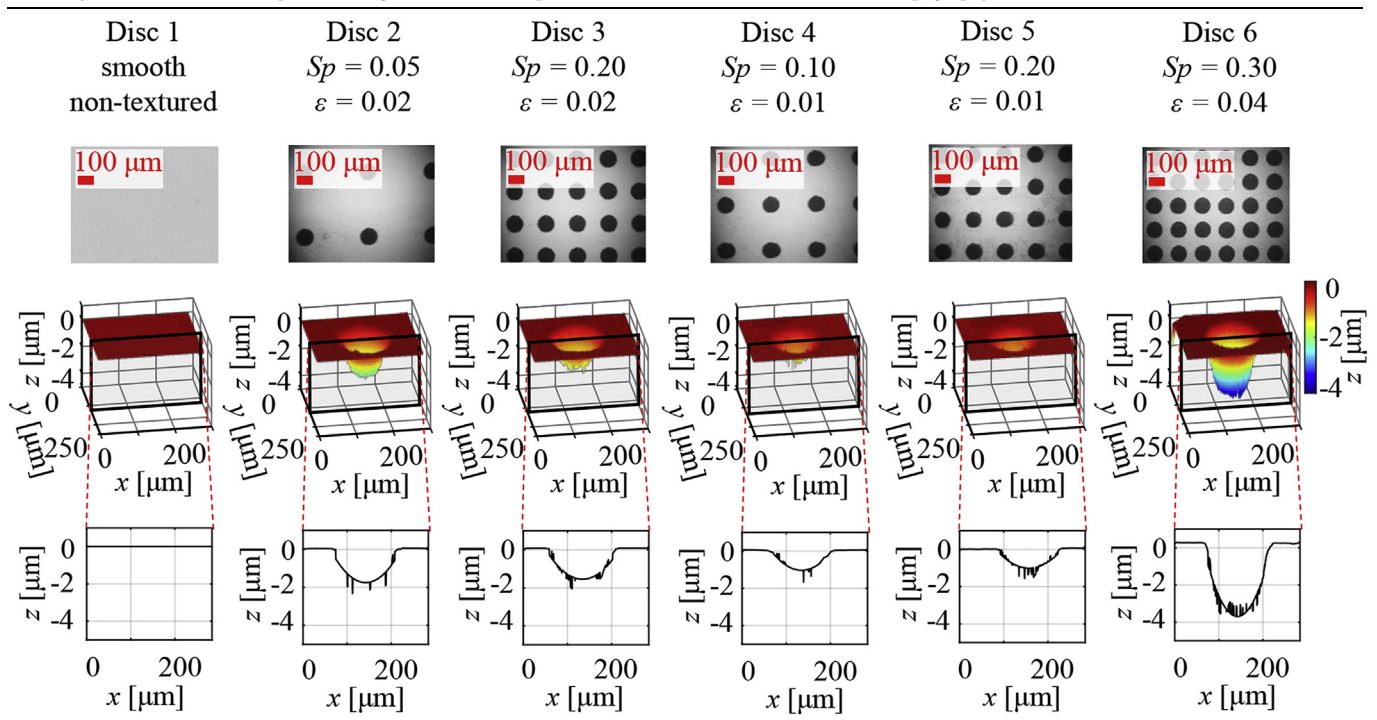
A virgin polyethylene pin (UHMWPE GUR 1050), and the surface topography of its flat articulating surface measured using white light interferometry.



Parameter	Value	Parameter	Value
R_a [μm]	3.58	n_s [$1/\mu\text{m}^2$]	0.50
R_q [μm]	3.64	σ_s [μm]	1.35
R_t [μm]	207.49	R_s [μm]	0.35

Table 2

CoCrMo discs with different microtexture designs, identified by the texture density S_p and texture aspect ratio ϵ . Optical microscopy and white light interferometry (with cross-sectional profile) images similar to our previous work [29], illustrate the surface topography of the discs.



similar to our previous work [29]. Note that no raised edges exist around the contour of the texture features resulting from material re-deposition during the LST process. Furthermore, the surface topography of the land area between the texture features remains unaltered by the LST process.

2.2. Pin-on-disc friction and wear measurement apparatus

Fig. 1 shows a schematic of a single-station POD friction and wear measurement apparatus, developed and built in our lab, which we use to measure the friction coefficient between polyethylene pins articulating with CoCrMo discs. POD experiments are widely used in the orthopedics field to evaluate different material pairs (pin and disc) as a

function of operating conditions, because it allows for fast, inexpensive screening compared to lengthy, costly hip simulator tests. This POD apparatus consists of a two degrees-of-freedom (DOF) motion mechanism with two electrical motors, which allows creating any kinematic cycle within the operating domain of the apparatus. The polyethylene pin is connected to a tri-axial force sensor using a pin holder, with a conical hole to fit the hemispherical end of the pin, which self-aligns the pin with the disc surface. The tri-axial force sensor measures the normal and tangential forces exerted on the pin. We use the tangential force on the pin to compute the friction coefficient between the articulating surfaces, and we use the normal force for force control of the pneumatic cylinder that maintains any pre-set contact pressure between the pin and disc.

2.3. Friction and wear measurement procedure

2.3.1. Short-duration friction coefficient measurements

We measure the friction coefficient of virgin polyethylene pins articulating with Discs 1–6 (see Table 2) using operating conditions selected based on the in-vivo operating conditions of prosthetic hip implants and the ASTM F732-17 standard for POD wear testing of polymeric materials used in joint prostheses [40]. ASTM F732-17 suggests using a contact pressure between 2 and 10 MPa, and the literature reports that the contact pressure between the articulating surfaces of an MOP prosthetic hip implant ranges between 1 to 12 MPa during normal gait [41–45]. On the other hand, Saikko et al. [46] recommend that the contact pressure in POD experiments evaluating prosthetic implant materials does not exceed 2.0 MPa to best mimic in-vivo mechanical behavior of a polyethylene acetabular liner. Hence, we perform POD experiments with a contact pressure between the pin and the disc ranging from 1 to 2 MPa. The pin follows a circular path of 10 mm diameter, resulting in a sliding distance of 31.4 mm per cycle; this is identical to the kinematics used in our earlier wear experiments [29], which is within the in-vivo sliding distance range (8.6–33.6 mm) documented in the literature [47], and is between 25 and 150 mm as

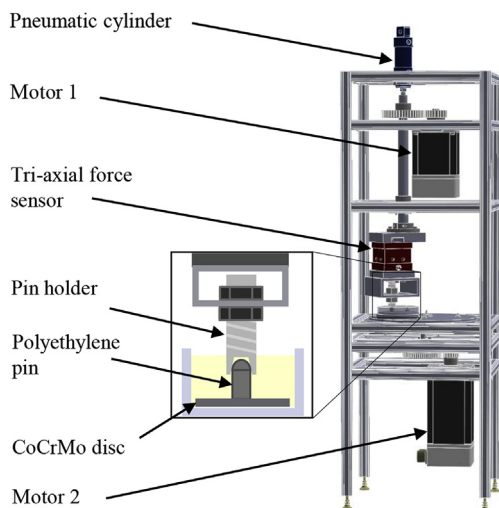


Fig. 1. Schematic of single-station POD tester. Inset shows detail of polyethylene pin articulating with CoCrMo disc.

suggested in ASTM F732-17 [40]. We select a cycle frequency between 1 to 2 Hz based on natural human gait as a function of age and gender [48–50], which also falls within the ASTM F732-17 recommended cycle frequency of 0.5–2 Hz. Additionally, we select Disc 1 and 4 for extended friction coefficient measurements with cycle frequency ranging from 0.1 to 2.2 Hz. We select Disc 1 (non-textured) as a benchmark, and Disc 4 represents a typical example of the microtextured CoCrMo discs, based on preliminary friction coefficient measurements.

Bovine serum (Hyclone, Logan, UT), with a protein concentration of 20 mg/ml, at room temperature floods the interface between the polyethylene pin and CoCrMo disc. We use the protocol of the ASTM F2025 standard [51] to clean both articulating surfaces prior to testing.

We measure the friction force between a virgin polyethylene pin and a CoCrMo disc using the tri-axial force sensor (4 kHz sampling frequency) for 20 s after each experiment reaches steady-state, and compute the average. We convert the force measurement to friction coefficient by calculating the ratio of the magnitude of the friction force vector tangential to the wear path using the X and Y force components of the tri-axial force sensor, and the magnitude of the normal force vector (Z force component of the tri-axial force sensor). We repeat each experiment three times and report the average, minimum, and maximum value.

2.3.2. Long-duration friction coefficient measurements

We perform 5-h duration friction coefficient measurements to study the friction coefficient of virgin polyethylene pins articulating with CoCrMo discs as a function of time and operating conditions. Disc 1 (non-textured) serves as the benchmark, whereas Disc 4 is representative of all microtextured CoCrMo discs, based on the short-term friction coefficient measurement results. We select the following two extreme sets of operating conditions based on patient age, body mass, and activity level: (1) 1 MPa contact pressure and 1.8 Hz cycle frequency, representing a young, fit patient with low body mass and an active lifestyle, and (2) 2 MPa contact pressure, and 1 Hz cycle frequency, representing an old, obese patient with sedentary lifestyle [42,43,49,50]. All other experimental parameters are the same as those used in the short-duration friction coefficient measurements (see section 2.3.1).

2.3.3. Correlation between the friction coefficient and polyethylene wear rate

We measure the short-duration friction coefficient of retrieved polyethylene pins from our previous wear experiments [29] articulating with Discs 2–6, to evaluate the correlation between polyethylene wear rate and friction coefficient. We use the same operating conditions as the wear experiments, i.e., 2 MPa contact pressure, 1 Hz cycle frequency, and a circular wear path with diameter of 10 mm, and submerge the interface between the pin and disc in bovine calf serum (Hyclone, Logan, UT) with 20 mg/ml protein concentration.

2.4. Data analysis

The null hypothesis is that microtexture design does not affect the average friction coefficient between the virgin polyethylene pins and CoCrMo discs, over the range of the operating conditions considered in the experiments. We test this null hypothesis with a student t -test for two-tailed distributions with unequal variance between the friction coefficient measurements of virgin polyethylene pins articulating with CoCrMo discs with different microtexture designs. We consider a p -value of 0.05 statistically significant, as commonly used in other experimental studies of orthopedic polyethylene materials [52], but also report the actual p -value. We use linear regression analysis to assess the relationship between the polyethylene wear rate of the retrieved polyethylene pins from our previous wear experiments [29] and friction coefficient measurements obtained in this study.

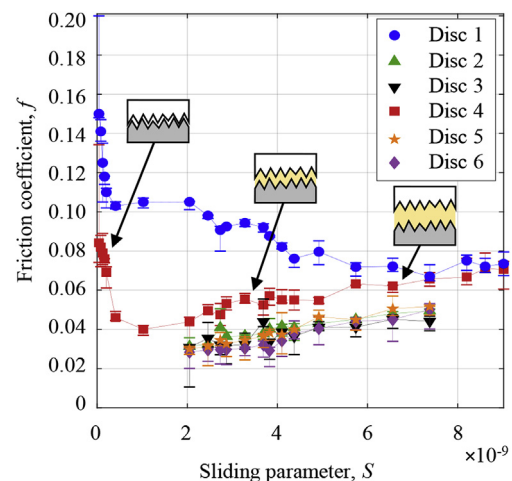


Fig. 2. Friction coefficient between the virgin polyethylene pins and the CoCrMo Discs 1–6 under in-vivo prosthetic hip implant operating conditions versus sliding parameter S .

3. Results and discussion

Fig. 2 shows the short-duration friction coefficient measurements between the virgin polyethylene pins and the CoCrMo Discs 1–6 under in-vivo prosthetic hip implant operating conditions (see section 2.3.1), and the extended operating conditions for Disc 1 and Disc 4, as a function of the sliding parameter S , defined as [53]:

$$S = \frac{\mu_d \cdot c}{p} \quad (1)$$

Here, $\mu_d = 4.1$ mPa s [54] is the dynamic viscosity of the lubricant, c is the cycle frequency, and p is the contact pressure between the sliding surfaces. The data points represent the average of three measurements, whereas the error bars indicate the minimum and maximum measurement. Fig. 2 shows that a virgin polyethylene pin articulating with Disc 1 (non-textured) results in a higher friction coefficient compared to articulating with Disc 2–6 (microtextured), independent of the microtexture design and operating conditions. Furthermore, we observe that under in-vivo prosthetic hip implant operating conditions, the friction coefficient increases with increasing S for all experiments with Disc 2–6, whereas it decreases with increasing S for Disc 1.

The lubrication mechanism between the polyethylene and CoCrMo bearing surfaces changes as a function of operating conditions as demonstrated by Stribeck [55]. The patterned microtexture creates microhydrodynamic bearings, which increases the lubricant film thickness for a constant external bearing load, illustrated by the insets in Fig. 2. This causes the lubrication regime to change from boundary/mixed lubrication for the non-textured Disc 1 to the elasto-hydrodynamic/hydrodynamic lubrication regime for the microtextured Discs 2–6, under constant operating conditions. In the boundary/mixed lubrication regime the bearing load is partially supported by the pressure in the lubricant film, and partially by solid-on-solid asperity contact between the pin and disc bearing surfaces. However, in the elasto-hydrodynamic/hydrodynamic lubrication regime, the bearing load is entirely borne by the pressure in the lubricant film and, thus, the friction coefficient is only dependent on the shear stress in the lubricant. The non-textured Disc 1 operates in the boundary/mixed lubrication regime, and increasing S , i.e., increasing the cycle frequency c or decreasing contact pressure p for constant lubricant viscosity μ_d , causes an increasing portion of the bearing load to be supported by pressure in the lubricant film as opposed to asperity contact. As such, the lubrication regime changes from boundary/mixed lubrication to elasto-hydrodynamic/hydrodynamic lubrication, thus decreasing the friction coefficient. On the other hand, the microtextured Discs 2–6 already operate in the

elastohydrodynamic/hydrodynamic lubrication regime and, thus, the lubricant shear rate increases with increasing sliding parameter S , which in turn slightly increases the friction coefficient. Specifically, we observe that Disc 4 ($S_p = 0.1$, $\varepsilon = 0.01$) consistently results in the highest friction coefficient among all microtextured discs, which we compute to be significantly different from the other discs ($1.25 \times 10^{-18} < p < 1.12 \times 10^{-14}$). The difference in friction coefficient between all other microtextured discs is not significant ($0.10 < p < 0.85$ for all other microtextured discs compared to each other). This indicates that the geometry of the shallow microtexture on Disc 4 performs best to increase the lubricant film thickness and reduce contact between the bearing surfaces, under the operating conditions used in this work.

To further verify that the Stribeck curve explains the physical behavior observed in these experiments, we perform friction coefficient measurements over an extended range of operating conditions, attempting to visualize the Stribeck curve for the non-textured Disc 1 and the microtextured Disc 4 (Fig. 2). We observe that for the microtextured Disc 4, the friction coefficient first decreases with increasing S , and then increases with increasing S , demonstrating a change from boundary/mixed to elastohydrodynamic/hydrodynamic lubrication. In contrast, the friction coefficient between the virgin polyethylene pin and Disc 1 monotonically decreases with increasing S , indicating that the non-textured Disc 1 operates in the boundary/mixed lubrication regime for the operating conditions considered in this work, because it lacks the microhydrodynamic bearings.

Fig. 3 shows long-duration friction coefficient measurements of virgin polyethylene pins articulating with Disc 1 and Disc 4 as a function of time, under two extreme in-vivo operating conditions (high and low-activity patient) as detailed in section 2.3.1. From Fig. 3 we observe that Disc 1 exhibits a higher friction coefficient for low S ($p = 2$ MPa, cycle frequency 1.0 Hz) than Disc 4. In contrast, Disc 4 exhibits a higher friction coefficient for high S ($p = 1$ MPa, cycle frequency 1.8 Hz) than Disc 1. Hence, Disc 1 operates in the boundary/mixed lubrication regime, where the friction coefficient decreases with increasing S , whereas Disc 4 operates in the elastohydrodynamic/hydrodynamic regime, where the friction coefficient increases with increasing S . Fig. 3 also shows that the friction coefficient decreases as a function of time for Disc 1 independent of the operating conditions, while it remains almost constant for Disc 4, especially at high S . Since the bearing load is partially borne by solid-on-solid asperity contact in the boundary/mixed lubrication regime, the polyethylene surface undergoes polishing because the asperities wear, thus reducing the friction coefficient. On

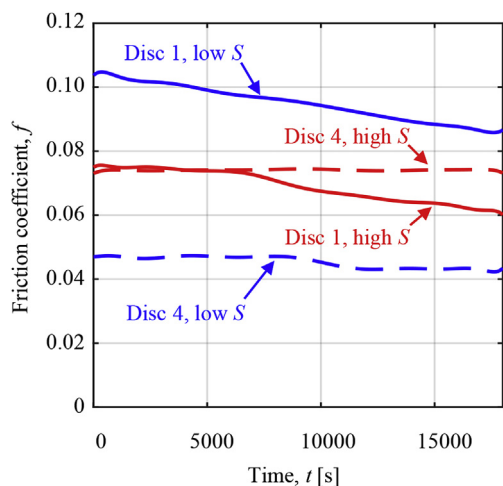


Fig. 3. Friction coefficient of virgin polyethylene pins articulating with Disc 1 and Disc 4 versus time, under two extreme in-vivo operating conditions: (1) contact pressure 2 MPa, cycle frequency 1.0 Hz (low S), and (2) contact pressure 1 MPa, cycle frequency 1.8 Hz (high S).

Table 3 Average surface roughness (R_a) of the polyethylene pin articulating surface before and after the long-term friction coefficient measurements.

	Low S			High S		
	$R_{a, \text{ before}}$ [μm]	$R_{a, \text{ after}}$ [μm]	ΔR_a	$R_{a, \text{ before}}$ [μm]	$R_{a, \text{ after}}$ [μm]	ΔR_a
Disc 1	4.45	2.94	–34%	5.48	3.77	–31%
Disc 4	3.58	2.99	–16%	3.58	3.41	–5%

the other hand, in the elastohydrodynamic/hydrodynamic lubrication regime, the bearing surfaces are separated by a lubricant film, and the friction coefficient is only dependent on the shear stress in the lubricant, which remains constant under constant operating conditions.

Table 3 shows the average surface roughness R_a of the articulating surface of the polyethylene pins used in Fig. 3 and the percent change of $\Delta R_a = (R_{a, \text{ before}} - R_{a, \text{ after}})/R_{a, \text{ before}}$ before and after the long-term friction coefficient measurements. The results of Table 3 show that the decrease of R_a is greater for the polyethylene pins articulating with Disc 1 than Disc 4, corroborating the findings shown in Fig. 3. The polyethylene pins articulating with Disc 1 operate in the boundary/mixed lubrication regime and are subject to wear and polishing, thus resulting in a larger change in the average surface roughness than the pins that articulate with Disc 4, which operate in the elastohydrodynamic/hydrodynamic lubrication regime, with almost no solid-on-solid contact between pin and disc. Additionally, the reduction of R_a is greater for the polyethylene pin that articulates with Disc 4 under low S , than for the polyethylene pin that articulates with Disc 4 under high S . In the elastohydrodynamic/hydrodynamic lubrication regime the lubricant film thickness increases with increasing S and, thus, it reduces the likelihood of asperity contact between pin and disc.

Fig. 4 shows the friction coefficient as a function of polyethylene wear rate for three types of retrieved polyethylene pins (GUR 1050 UHMWPE, HXPE, and VEXPE) articulating with microtextured CoCrMo discs (Discs 2–6). We also show the linear regression and R-squared (R^2) value computed for each retrieved polyethylene pin type. Our earlier work [29] documents the details of the polyethylene wear experiments, where the loading conditions are identical to those of the friction coefficient experiments used here. Fig. 4 shows that the polyethylene wear rate is inversely related to the friction coefficient of the retrieved polyethylene pins after 2 million wear cycles. Hence, it demonstrates that under elastohydrodynamic/hydrodynamic lubrication, a higher

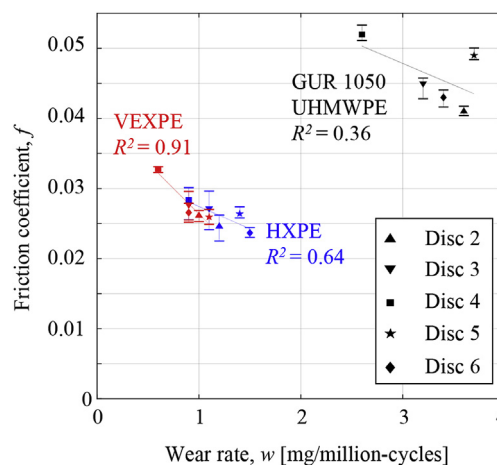


Fig. 4. Friction coefficient as a function of polyethylene wear rate for three types of retrieved polyethylene pins after 2 million wear cycles (GUR 1050 UHMWPE, HXPE, and VEXPE) articulating with microtextured CoCrMo discs in the elastohydrodynamic/hydrodynamic lubrication regime. Linear regression and R^2 value calculated for each retrieved polyethylene pin type is also shown.

friction coefficient between the articulating pin and disc indicates a greater lubricant film thickness, which in turn reduces asperity contact and polyethylene wear.

We also observe that R^2 decreases with increasing wear rate. This is likely because polyethylene pins articulating with different micro-textured discs do not wear identically. For instance, a GUR 1050 UHMWPE pin that articulates with Disc 5 (highest wear rate) shows $R_{a, after} = 11.74 \mu\text{m}$, which is almost four times that of a GUR 1050 UHMWPE pin that articulates with Disc 4 (lowest wear rate), i.e., $R_{a, after} = 3.23 \mu\text{m}$. Additionally, the range of R_a values of the polyethylene articulating surface after 2 million wear cycles is different for UHMWPE, HXPE, and VEXPE pins. For instance, $R_{a, after} = 9.69 \mu\text{m}$ and $R_{a, after} = 5.03 \mu\text{m}$ for the VEXPE pins articulating with Disc 5 and Disc 4 pins, respectively. Furthermore, other wear mechanisms, such as fatigue wear, have a more substantial effect on the total polyethylene wear rate at the later stages of wear, especially for UHMWPE GUR 1050, since it has lower fatigue resistance compared to VEXPE and HXPE pins [52]. As such, the friction coefficient may be a good analog for the polyethylene wear rate at the early stages of wear and with a low wear rate. However, for high wear rates, or as wear accumulates, the instantaneous friction coefficient measurement does not represent the total wear rate accurately.

The primary limitations of the friction coefficient experiments documented in this study are related to POD testing. The human hip has a complex geometry that cannot be represented by the simplified flat-on-flat geometry of POD testing. Furthermore, the static loading used in this work does not simulate the dynamic in-vivo loading on the human hip, as well as occasional spikes in hip contact pressure resulting from other activities rather than regular walking gait, such as jumping and climbing of stairs. The POD tester has a limited number of degrees-of-freedom compared to the human hip, so it cannot accurately mimic the in-vivo human hip kinematics. Another important factor is the smaller contact area of the polyethylene pin compared to the polyethylene acetabular liner of the prosthetic hip implants. Contact area has been shown to have a direct effect on the polyethylene wear rate and friction [46,56]. Despite these limitations, POD testing is useful for fast and inexpensive screening of new materials, prior to performing costly and time-consuming hip simulator testing. The results presented here demonstrate potential of using a patterned microtexture to reduce friction and wear in metal-on-polyethylene hip implants, and using the patterned microtexture design as a means of tuning the performance of the articulating surface to different operating conditions. Although this study showed promising results, experiments with more sophisticated hip joint simulator and in-vivo experiments are required to confirm our results.

4. Conclusion

We show that the lubrication regime between a polyethylene pin and a CoCrMo disc, under operating conditions relevant to in-vivo prosthetic hip implants, changes from boundary/mixed lubrication to elastohydrodynamic/hydrodynamic lubrication by manufacturing a patterned microtexture of shallow concave “dimples” on the surface of the CoCrMo disc.

We demonstrate, by combining friction coefficient and surface topography measurements, that one microtexture geometry design, Disc 4 ($S_p = 0.1$, $\epsilon = 0.01$), consistently results in the highest lubricant film thickness compared to all other microtexture designs and the entire range of operating conditions used in this work.

In the context of patient-specific prosthetic hip implant design, we conclude that a patterned microtexture can benefit the longevity of hip implants for high-activity patients with low body mass when high S operating conditions exist, which enables creating elastohydrodynamic/hydrodynamic lubrication, as opposed to when low S operating conditions exist, typically found in high body mass, low-activity patients. More sophisticated experiments using hip joint simulators are

needed to translate the results documented here to commercial implants.

Correlating wear data from our previous work with friction coefficient data from this study also shows that instantaneous friction coefficient measurements do not accurately represent the cumulative polyethylene wear rate in POD wear experiments.

Acknowledgments

A.B. and B.R. acknowledge support from the National Institutes of Health, National Institute of Arthritis and Musculoskeletal and Skin Diseases under grant 1R03AR066826-01A1.

References

- [1] Foran J. Total Hip Replacement - OrthoInfo - AAOS n.d. <https://orthoinfo.aaos.org/en/treatment/total-hip-replacement> (accessed March 25, 2018).
- [2] Ong KL, Lau E, Suggs J, Kurtz SM, Manley MT. Risk of subsequent revision after primary and revision total joint arthroplasty. *Clin Orthop Relat Res* 2010;468:3070–6. <https://doi.org/10.1007/s11999-010-1399-0>.
- [3] Hallab NJ, Jacobs JJ. Chemokines associated with pathologic responses to orthopedic implant debris. *Front Endocrinol (Lausanne)* 2017;8:5. <https://doi.org/10.3389/fendo.2017.00005>.
- [4] Badarudeen S, Shu AC, Ong KL, Baykal D, Lau E, Malkani AL. Complications after revision total hip arthroplasty in the medicare population. *J Arthroplasty* 2017;32:1954–8. <https://doi.org/10.1016/j.arth.2017.01.037>.
- [5] Holt G, Murnaghan C, Reilly J, Meek RMD. The biology of aseptic osteolysis. *Clin Orthop Relat Res* 2007;460:240–52. <https://doi.org/10.1097/BLO.0b013e31804b4147>.
- [6] Guo L, Yang YY, An B, Yang YY, Shi L, Han X, et al. Risk factors for dislocation after revision total hip arthroplasty: a systematic review and meta-analysis. *Int J Surg* 2017;38:123–9.
- [7] Sadoghi P, Liebensteiner M, Agreiter M, Leithner A, Böhler N, Labek G. Revision surgery after total joint arthroplasty: a complication-based analysis using worldwide arthroplasty registers. *J Arthroplasty* 2013;28:1329–32.
- [8] Matziolis G, Krakow L, Layher F, Sander K, Bossert J, Brodt S. Patient-specific contact stress does not predict polyethylene wear rate in a specific pressfit cup. *J Arthroplasty* 2017;32:3802–5. <https://doi.org/10.1016/j.arth.2017.07.027>.
- [9] Takada R, Jinno T, Koga D, Hirao M, Muneta T, Okawa A. Comparison of wear rate and osteolysis between annealed and remelted highly cross-linked polyethylene in total hip arthroplasty. A case control study at 7 to 10 years follow-up. *Orthop Traumatol Surg Res* 2016;102:717–21. <https://doi.org/10.1016/j.OTS.2016.04.010>.
- [10] Dobzyniak M, Fehring TK, Odum S. Early failure in total hip arthroplasty. *Clin Orthop Relat Res* 2006;447:76–8. <https://doi.org/10.1097/01.blo.0000203484.90711.52>.
- [11] Kurtz SM, Ong KL, Schmier J, Mowat F, Saleh K, Dybvik E, et al. Future clinical and economic impact of revision total hip and knee arthroplasty. *J Bone Jt Surg* 2007;89:144. <https://doi.org/10.2106/JBJS.G.00587>.
- [12] Kurtz S, Patel J. The clinical performance of highly cross-linked UHMWPE in hip replacements. *UHMWPE biomater. Handb. Elsevier*; 2015. p. 57–71.
- [13] Kurtz SM, Gawel HA, Patel JD. History and systematic review of wear and osteolysis outcomes for first-generation highly crosslinked polyethylene. *Clin Orthop Relat Res* 2011;469:2262–77. <https://doi.org/10.1007/s11999-011-1872-4>.
- [14] Doshi B, Ward JS, Oral E, Muratoglu OK. Fatigue toughness of irradiated vitamin E/UHMWPE blends. *J Orthop Res* 2016;34:1514–20. <https://doi.org/10.1002/jor.23168>.
- [15] Oral E, Neils AL, Doshi BN, Fu J, Muratoglu OK. Effects of simulated oxidation on the in vitro wear and mechanical properties of irradiated and melted highly crosslinked UHMWPE. *J Biomed Mater Res B Appl Biomater* 2016;104:316–22. <https://doi.org/10.1002/jbm.b.33368>.
- [16] Nebergall AK, Troelsen A, Rubash HE, Malchau H, Rolfson O, Greene ME. Five-year experience of vitamin e-diffused highly cross-linked polyethylene wear in total hip arthroplasty assessed by radiostereometric analysis. *J Arthroplasty* 2016;31:1251–5. <https://doi.org/10.1016/j.arth.2015.12.023>.
- [17] Ruggiero A, D'Amato R, Gómez E, Merola M. Experimental comparison on tribological pairs UHMWPE/TiAL6V4 alloy, UHMWPE/AISI316L austenitic stainless and UHMWPE/AL2O3 ceramic, under dry and lubricated conditions. *Tribol Int* 2016;96:349–60. <https://doi.org/10.1016/j.triboint.2015.12.041>.
- [18] Lachiewicz PF, Kleeman LT, Seyler T. Bearing surfaces for total hip arthroplasty. *J Am Acad Orthop Surg* 2018;26:45–57. <https://doi.org/10.5435/JAAOS-D-15-00754>.
- [19] Yang Y, Ong JL, Tian J. Deposition of highly adhesive ZrO2 coating on Ti and CoCrMo implant materials using plasma spraying. *Biomaterials* 2003;24:619–27. [https://doi.org/10.1016/S0142-9612\(02\)00376-9](https://doi.org/10.1016/S0142-9612(02)00376-9).
- [20] Sonohata M, Kitajima M, Kawano S, Mawatari M. Wear of XLPE liner against zirconium heads in cementless total hip arthroplasty for patients under 40 Years of age. *HIP Int* 2017;27:532–6. <https://doi.org/10.5301/hipint.5000513>.
- [21] Olsson J, Grehk TM, Berling T, Persson C, Jacobson S, Engqvist H. Evaluation of silicon nitride as a wear resistant and resorbable alternative for total hip joint replacement. *Biomater* 2012;2:94–102. <https://doi.org/10.4161/biom.20710>.

- [22] Aherwar A, Patnaik A, Bahraminasab M, Singh A. Preliminary evaluations on development of new materials for hip joint femoral head. *Proc Inst Mech Eng Part L J Mater Des Appl* 2017;146442071771449. <https://doi.org/10.1177/1464420717714495>.
- [23] Affatato S, Ruggiero A, Merola M. Advanced biomaterials in hip joint arthroplasty. A review on polymer and ceramics composites as alternative bearings. *Compos B Eng* 2015;83:276–83. <https://doi.org/10.1016/j.compositesb.2015.07.019>.
- [24] Sawano H, Warisawa SS, Ishihara S. Study on long life of artificial joints by investigating optimal sliding surface geometry for improvement in wear resistance. *Precis Eng* 2009;33:492–8.
- [25] Ito H, Kaneda K, Yuhta T, Nishimura I, Yasuda K, Matsuno T. Reduction of polyethylene wear by concave dimples on the frictional surface in artificial hip joints. *J Arthroplasty* 2000;15:332–8. [https://doi.org/10.1016/S0883-5403\(00\)90670-3](https://doi.org/10.1016/S0883-5403(00)90670-3).
- [26] Dong Y, Svoboda P, Vrbka M, Kostal D, Urban F, Cizek J, et al. Towards near-permanent CoCrMo prosthesis surface by combining micro-texturing and low temperature plasma carburising. *J Mech Behav Biomed Mater* 2016;55:215–27. <https://doi.org/10.1016/j.jmbbm.2015.10.023>.
- [27] Cho M, Choi H-J. Optimization of surface texturing for contact between steel and ultrahigh molecular weight polyethylene under boundary lubrication. *Tribol Lett* 2014;56:409–22. <https://doi.org/10.1007/s11249-014-0418-9>.
- [28] Chyr A, Qiu M, Speltz JW, Jacobsen RL, Sanders AP, Raeymaekers B. A patterned microtexture to reduce friction and increase longevity of prosthetic hip joints. *Wear* 2014;315:51–7.
- [29] Borjali A, Langhorn J, Monson K, Raeymaekers B. Using a patterned microtexture to reduce polyethylene wear in metal-on-polyethylene prosthetic bearing couples. *Wear* 2017;392–393:77–83. <https://doi.org/10.1016/j.wear.2017.09.014>.
- [30] Langhorn J, Borjali A, Hippensteel E, Nelson W, Raeymaekers B. Microtextured CoCrMo alloy for use in metal-on-polyethylene prosthetic joint bearings: multi-directional wear and corrosion measurements. *Tribol Int* 2018;124:178–83. <https://doi.org/10.1016/j.triboint.2018.04.007>.
- [31] Oberg T, Karsznia A, Oberg K. Basic gait parameters: reference data for normal subjects, 10–79 years of age. *J Rehabil Res Dev* 1993;30:210–23. <https://doi.org/10.1080/19397030902947041>.
- [32] Chehab EF, Andriacchi TP, Favre J. Speed, age, sex, and body mass index provide a rigorous basis for comparing the kinematic and kinetic profiles of the lower extremity during walking. *J Biomech* 2017;58:11–20. <https://doi.org/10.1016/j.jbiomech.2017.04.014>.
- [33] Rodgers MM. Dynamic foot biomechanics. *J Orthop Sports Phys Ther* 1995;21:306–16. <https://doi.org/10.2519/jospt.1995.21.6.306>.
- [34] Yoneyama M, Mitoma H, Hayashi A. Effect of age, gender, and walkway length on accelerometry-based gait parameters for healthy adult subjects. *J Mech Med Biol* 2016;16:1650029. <https://doi.org/10.1142/S0219519416500299>.
- [35] Tackson SJ, Krebs DE, Harris BA. Acetabular pressures during hip arthritis exercises. *Arthritis Care Res (Hoboken)* 1997;10:308–19. <https://doi.org/10.1002/art.1790100505>.
- [36] Qiu M, Chyr A, Sanders AP, Raeymaekers B. Designing prosthetic knee joints with bio-inspired bearing surfaces. *Tribol Int* 2014;77:106–10.
- [37] ASTM F648-14. Standard specification for ultra-high-molecular-weight polyethylene powder and fabricated form for surgical implants. West Conshohocken, PA: ASTM International; 2014. www.astm.org.
- [38] Pawar G, Pawlus P, Etsion I, Raeymaekers B. The effect of determining topography parameters on analyzing elastic contact between isotropic rough surfaces. *J Tribol* 2012;135. <https://doi.org/10.1115/1.4007760>.
- [39] ASTM F1537-08. Standard specification for wrought Cobalt-28Chromium-6Molybdenum alloys for surgical implants (UNS R31537, UNS R31538, and UNS R31539). West Conshohocken, PA: ASTM International; 2008. www.astm.org.
- [40] ASTM F732-17. Standard test method for wear testing of polymeric materials used in total joint prostheses. West Conshohocken, PA: ASTM International; 2017. www.astm.org.
- [41] Hua X, Li J, Jin Z, Fisher J. The contact mechanics and occurrence of edge loading in modular metal-on-polyethylene total hip replacement during daily activities. *Med Eng Phys* 2016;38:518–25. <https://doi.org/10.1016/j.medengphy.2016.03.004>.
- [42] Bergmann G, Bender A, Dymke J, Duda G, Damm P. Standardized loads acting in hip implants. *PLoS One* 2016;11:e0155612. <https://doi.org/10.1371/journal.pone.0155612>.
- [43] Damm P, Kutzner I, Bergmann G, Rohlmann A, Schmidt H. Comparison of in vivo measured loads in knee, hip and spinal implants during level walking. *J Biomech* 2017;51:128–32. <https://doi.org/10.1016/j.jbiomech.2016.11.060>.
- [44] Houcke J, Khanduja V, Pattyn C, Audenaert E. The history of biomechanics in total hip arthroplasty. *Indian J Orthop* 2017;51:359. <https://doi.org/10.4103/ortho.IJOrtho.280.17>.
- [45] Tackson SJ, Krebs DE, Harris BA. Acetabular pressures during hip arthritis exercises. *Arthritis Care Res* 1997;10:308–19.
- [46] Saikko V. Effect of contact pressure on wear and friction of ultra-high molecular weight polyethylene in multidirectional sliding. *Proc Inst Mech Eng Part H J Eng Med* 2006;220:723–31. <https://doi.org/10.1243/09544119JEIM146>.
- [47] Bennett D, Humphreys L, O'Brien S, Kelly C, Orr J, Beverland DE. The influence of wear paths produced by hip replacement patients during normal walking on wear rates. *J Orthop Res* 2008;26:1210–7. <https://doi.org/10.1002/jor.20583>.
- [48] Aikaterini TP. Ji. Frequency and velocity of people walking - articles - the institution of structural engineers. *Struct Eng* 2005:83.
- [49] Himann JE, Cunningham DA, Rechnitzer PA, Paterson DH. Age-related changes in speed of walking. *Med Sci Sports Exerc* 1988;20:161–6.
- [50] Oberg T, Karsznia A, Oberg K. Basic gait parameters: reference data for normal subjects, 10–79 years of age. *J Rehabil Res Dev* 1993;30:210–23.
- [51] ASTM F2025-06. Standard practice for gravimetric measurement of polymeric components for wear assessment vol. 2012. West Conshohocken, PA: ASTM International; 2012. www.astm.org.
- [52] Oral E, Christensen SD, Malhi AS, Wannomae KK, Muratoglu OK. Wear resistance and mechanical properties of highly cross-linked, ultrahigh-molecular weight polyethylene doped with vitamin e. *J Arthroplasty* 2006;21:580–91. <https://doi.org/10.1016/j.arth.2005.07.009>.
- [53] Mathew Mate C. *Tribology on the small scale: a bottom up approach to friction, lubrication, and wear*. Oxford university press; 2008.
- [54] Chatterjee A. Intrinsic viscosity measurements of bovine serum albumin at different temperatures. *Nature* 1965;205. <https://doi.org/10.1038/205386a0>. 386–386.
- [55] Stribeck R. Characteristics of plain and roller bearings. *Zeit Ver Deut Ing* 1902;46:1463–70.
- [56] Mazzucco D, Spector M. Effects of contact area and stress on the volumetric wear of ultrahigh molecular weight polyethylene. *Wear* 2003;254:514–22. [https://doi.org/10.1016/S0043-1648\(03\)00135-2](https://doi.org/10.1016/S0043-1648(03)00135-2).